研究紹介

表面科学 Vol. 35, No. 9, pp. 486-491, 2014
特集「水の表面化学　―水を操る―」

MgO 超薄膜表面における水分子の分解反応の制御

鄭載勲[1]・申炯畯[2]・川合眞紀[3]・金有洙[1]

[1]理化学研究所 Kim 表面界面科学研究室　〒351-0198　埼玉県和光市広沢 2-1
[2]School of Mechanical and Advanced Materials Engineering, Ulsan National Institute of Science and Technology (UNIST), 100 Banyeon-ri, Eonyang, Ulju-gun, Ulsan 689-798, Republic of Korea
[3]東京大学大学院新領域創成科学研究科　〒277-8561　千葉県柏市柏の葉 5-1-5

（2014 年 5 月 21 日受付；2014 年 6 月 30 日掲載決定）

Controlling Dissociation Reaction of a Water Molecule on Ultrathin MgO Film

Jaehoon Jung[1], Hyung-Joon Shin[2], Maki Kawai[3] and Yousoo Kim[1]

[1]Surface and Interface Science Laboratory, RIKEN, 2-1 Hirosawa, Wako, Saitama 351-0198
[2]School of Mechanical and Advanced Materials Engineering, Ulsan National Institute of Science and Technology (UNIST), 100 Banyeon-ri, Eonyang, Ulju-gun, Ulsan 689-798, Republic of Korea
[3]Department of Advanced Materials Science, The University of Tokyo, 5-1-5 Kashiwanoha, Kashiwa, Chiba 277-8561

(Received May 21, 2014 ; Accepted June 30, 2014)

We have recently intensively studied the dissociation of individual water molecules on ultrathin MgO film grown on Ag(100) substrate at the single-molecule level, by means of both scanning tunneling microscopy experiment and density functional theory calculations. We have found clear evidence for that the chemical reactivity of ultrathin MgO film can be controlled by the film thickness, in which the interfacial interaction between oxide and metal substrate plays an important role in determining chemical reactivity. In this short review, we briefly discuss the role of the ultrathin insulating film in water dissociation induced by vibrationally excited state using inelastic tunneling electrons, which is crucial to selectively achieve two kinds of dissociation path, as well as underlying thickness dependence of chemical reactivity.

KEYWORDS : water dissociation, ultrathin insulating film, scanning tunneling microscopy, density functional theory

1. Introduction

Ultrathin oxide films grown on metal substrate have attracted a great deal of attention not only as supporting materials for chemically active species but also as catalysts itself.[1,2] In particular, significant efforts have been devoted to achieve high controllability using ultrathin oxide films because they provide noble dimensionality, i.e., film thickness, as a controllable parameter compared to their bulk counterparts. **Fig. 1** presents the suggested approaches to control the surface reactivity of ultrathin oxide films : (1) the charge redistribution between oxide-

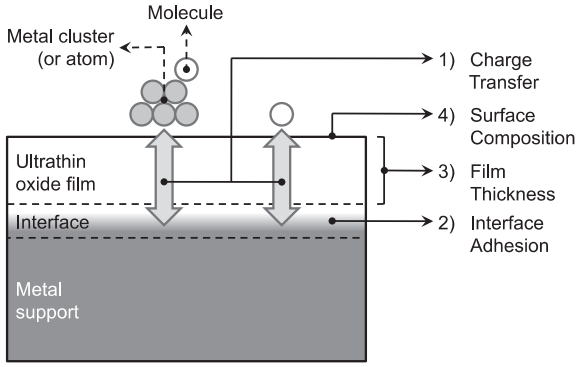

Fig. 1. Schematic diagram for the approaches to control the surface reactivity of ultrathin oxide film supported by a metal substrate. Adapted with permission from Ref. 8). Copyright 2012 American Chemical Society.

E-mail : ykim@riken.jp
E-mail : maki@t-u.tokyo.ac.jp

metal interface and adsorbates related to both work-function reduction due to oxide film and high electron affinity (EA) of adsorbates ; [3~5] (2) the enhancement of adhesion strength with polaronic distortion at the oxide-metal interface ; [6~8] (3) the film thickness closely associated with both the charging of adsorbates and interface adhesion ; [4, 6, 9] (4) the change in oxygen composition of polar oxide film relying on the ambient oxygen concentration.[10]

Recently, we have intensively studied the dissociation of individual H_2O molecules on ultrathin MgO film grown on Ag(100) substrate at the single-molecule level, by means of both scanning tunneling microscopy (STM) experiment and density functional theory (DFT) calculations.[6~9] Water dissociation is an issue not only of importance due to an elementary process for hydrogen generation[11] but also of fundamental scientific interest.[12] We successfully demonstrated that the two different dissociation pathways of individual H_2O molecules ($H_2O \rightarrow O^{2-} + 2H^+$ or $OH^- + H^+$) on MgO/Ag (100) can be selectively chosen by controlling tunneling bias voltage, which is closely related to the electronic decoupling of adsorbate from underneath metal substrate due to the insulating nature of oxide film.[9] In addition, we found undoubted evidence for that the chemical reactivity of ultrathin MgO film can be tuned by the film thickness. We disclosed that the change in adhesion strength accompanied with the interfacial electronic structure is crucial for resolving the dependence of chemical reactivity on the film thickness, which is not influenced by the charge redistribution between oxide-metal interface and adsorbates because of the low EA of adsorbates[6] (see (2) and (3) in Fig. 1). Based on our interpretation, we have recently proposed that introducing the local imperfections, such as an oxygen vacancy, and an oxygen or magnesium impurity, at the oxide-metal interface can be utilized in controlling the chemical reactivity of the ultrathin oxide film.[7] Our further extended study on interface engineering using 3d transition metal (TM) dopants (D_{TM} = Sc～Zn) for water dissociation on two-monolayer (ML) MgO film supported by Ag (100) substrate suggested that the chemical reactivity of an ultrathin oxide film grown on metal substrate can be systematically tailored and can also be explained ligand field effect, i.e., the interaction between the dopant and the oxide layer, at the interface.[8]

In this short review, we briefly discuss the role of the ultrathin insulating film in water dissociation induced by vibrationally excited state using inelastic tunneling electrons, which is crucial to selectively achieve two kinds of dissociation path, as well as underlying dependence of chemical reactivity on film thickness.

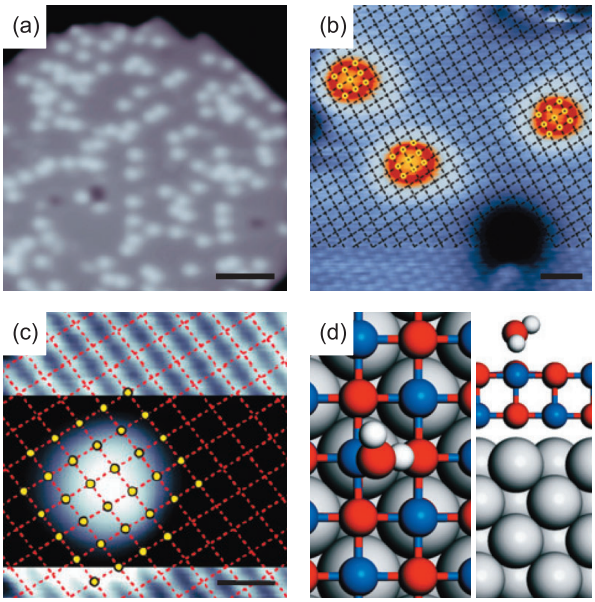

Fig. 2. (color online). STM image of H_2O molecules on (a) a 3-ML MgO/Ag (100) (V_s = 100 mV, I_t = 0.3 nA, Scale bar (S) = 5 nm) and (b) a 2-ML MgO (V_s = 100 mV, I_t = 0.3 nA, S = 1 nm). (c) STM image of a H_2O molecule on 3-ML-thick MgO (top and bottom region : V_s = 3 mV and I_t = 1.0 nA, middle region : V_s = 50 mV and I_t = 0.15 nA, and S = 0.5 nm). The dots in (b) and (c) represent the location of the Ag atoms underneath MgO film. (d) Top (left) and side (right) views of the optimized structure of isolated H_2O molecule adsorbed on a 2-ML MgO/Ag(100). Reprinted with permission from Ref 9). Copyright 2010 Macmillan Publishers.

2. State-Selective Dissociation of a Single Water Molecule on an Ultrathin MgO Film

We performed the study on water molecules on ultrathin MgO films grown on a Ag(100) substrate using STM at low temperatures.[9] **Fig. 2** a shows an STM image of isolated H_2O molecules on an MgO island. We can obtain stable STM images of H_2O molecules only at a relatively low bias (<200 mV) inside the MgO band gap using STM, otherwise H_2O molecules diffuse away on the film surface even at 4.7 K. Atomically resolved STM images acquired at a low bias show the positions of silver atoms beneath the film due to negligible density of states (DOS) of MgO film, in which the corresponding positions are either anion (O^{2-}) or cation (Mg^{2+}) sites of MgO, depending

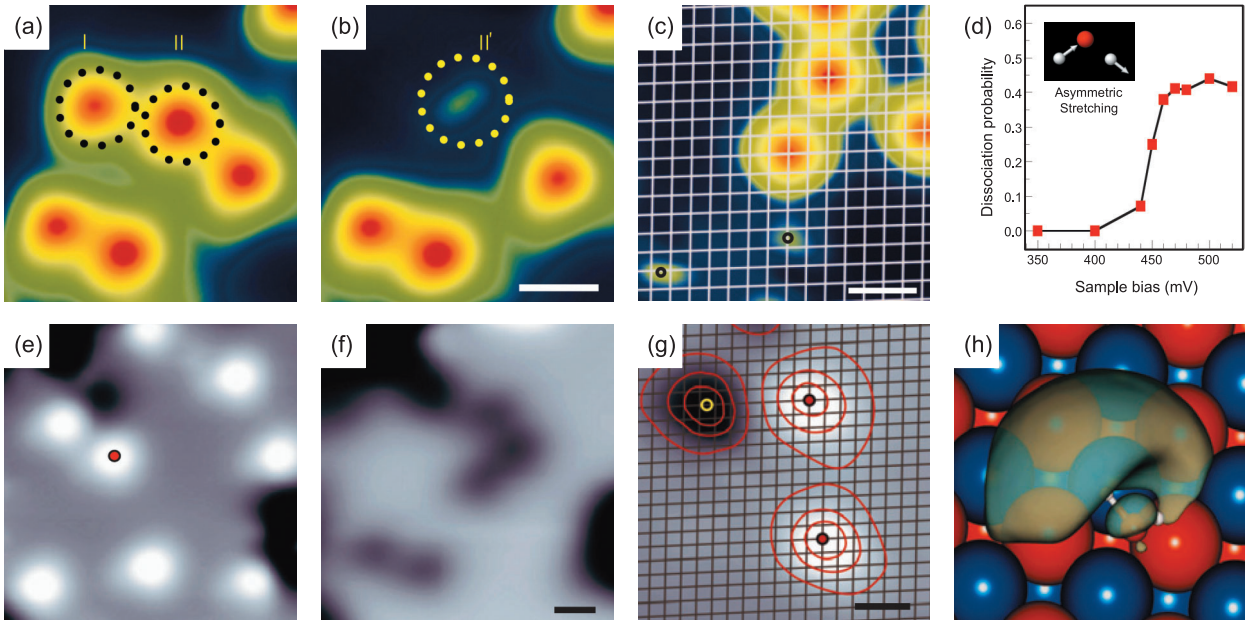

Fig. 3. (color online). STM images of H_2O molecules (a) before and (b) after applying bias voltage of 460 nm with tunneling currents of 3 and 5 nA onto I and II, respectively, on 2-ML MgO/Ag(100) ($V_s = 50$ mV, $I_t = 0.3$ nA, $S = 1$ nm). (c) STM image of H_2O molecules and dissociation products ($V_s = 50$ mV, $I_t = 0.3$ nA, $S = 1$ nm). Grid points correspond to the positions of Mg^{2+} ions. (d) The dissociation probability of isolated water molecules, which is derived from the ratio of the number of dissociated H_2O molecules to the total trial numbers (~20) at each bias voltage ($I_t = 5$ nA, pulse duration = 400 μs). STM images (e) before and (f) after dissociating H_2O molecules ($V_s = 100$ mV, $I_t = 0.3$ nA, $S = 1$ nm). A sample bias of 1.5 V was applied at the red mark in (e). (g) STM image of water (protrusions) and oxygen (depression) on 2-ML MgO/Ag(100) ($V_s = 100$ mV, $I_t = 0.5$ nA, $S = 1$ nm). The yellow and red circles indicate the adsorption sites of oxygen and water, respectively. The red lines are iso-profile contours of every 10 pm. (h) Charge density distribution for the LUMO of H_2O molecule on MgO film. Reprinted with permission from Ref 9). Copyright 2010 Macmillan Publishers.

on the film thickness.[13] Fig. 2 b shows a STM image of isolated H_2O molecules adsorbed on MgO films of 2-ML thickness. They adsorb at ontop sites of the Ag(100) surface underneath the 2-ML MgO film, which are corresponding to Mg^{2+} sites of the (100) facet of MgO film. On the 3-ML MgO film, H_2O molecules adsorb at the hollow sites of Ag(100) surface, which are also corresponding to the position of Mg^{2+} on the MgO(100) surface (Fig. 2 c). Our DFT calculations resulted in the optimized adsorption structure of an isolated H_2O molecule as shown in Fig. 2 d. The oxygen atom and one hydrogen atom of the H_2O molecule interact with an Mg^{2+} cation and its neighboring O^{2-} anion, respectively.

To induce the chemical reaction via inelastic electron tunneling (IET) process,[14, 15] we applied a bias voltage of 460 mV to two H_2O molecules I and II, respectively, on 2-ML MgO/Ag(100) (**Fig. 3** a). As a result, H_2O molecule I desorbed from the MgO film, whereas molecule II dissociated into the product II' (Fig. 3 b). The adsorption position of dissociated products is always the bridge site of (100) facet of MgO film (Fig. 3 c), which were identified to be hydroxyl species, i.e., $H_2O \rightarrow OH^- + H^+$, by DFT calculations. Similar to hydroxyl species, oxygen adatoms can also adsorb at the bridge sites on (100) facet of MgO film. However, they appear as depressions in the STM image obtained from the dissociation of O_2 molecules. The measured dissociation probability as a function of sample bias shown in Fig. 3 d reveals that the asymmetric OH stretching mode (ν_{OH}) is closely associated with the dissociation of water. In addition, it should be noted that we could not induce the dissociation of water molecule via vibrational excitation on 3-ML MgO/Ag(100) unlike 2-ML film, of which the thickness dependence will be discussed in next section.

We can also dissociate H_2O molecules by applying a bias voltage corresponding to the lowest unoccupied molecular orbital (LUMO) energy of adsorbate on MgO/Ag(100), which was evaluated to be 1.55 eV from DFT calculation. Applying a bias voltage of 1.5 V to the water molecules on 2-ML MgO/Ag(100) (Fig. 3 e) dissociated them into products (Fig. 3 f).

Appearance of the dissociated products, i.e., depression, is different from those of the hydroxyl, i.e., protrusion, which we observed in Fig. 3 b. We assigned these species to oxygen, because the adsorption positions of the products are the bridge sites of (100) facet of MgO film (Fig. 3 g), as confirmed by DFT calculations and by the STM measurement for the dissociation products of oxygen molecules on the MgO film. The charge density for the LUMO of H_2O molecule, obtained by DFT calculation, shows the anti-bonding character of OH bonds (Fig. 3 h), which is consistent with entire fragmentation, i.e., $H_2O \rightarrow O^{2-} + 2H^+$, of H_2O molecule.

Therefore, our results provide two different strategies for dissociating a water molecule, in which either the vibrational states or the electronic states of the molecule was utilized as a dissociation channel, depending on the applied bias voltage. Furthermore, the different dissociation products were obtained according to the reaction pathways as shown below.

Path(1) : $H_2O \rightarrow OH^- + H^+$ (ν_{OH}, 0.46 V)

Path(2) : $H_2O \rightarrow O^{2-} + 2H^+$ (LUMO, 1.5 V)

Whereas the dissociation of water via excitation of electronic states has also been demonstrated on various metal surfaces,[16, 17] the water dissociation via vibrational excitation has not been achieved thus far on a metal surface. The calculated dissociation barrier of water on the MgO film (770 meV) is smaller than the LUMO energy of 1.55 eV but is quite larger than the observed threshold energy of 448 meV corresponding to (ν_{OH}) as shown in Fig. 3 d. Therefore, in order to overcome the dissociation barrier by the excitation of the ν_{OH} mode, the energy of at least two electron processes is required. What is the driving force for the dissociation of H_2O molecules with much lower energy on the MgO film? Due to the electronic decoupling resulted from the insulating effect of the MgO layer, the lifetime of an electron in the molecular resonant state can be significantly elongated compared to that on metal substrate.[18] Thus, the IET process should be far more effective on an insulating film than on metal substrates.[19] As a result, direct multiple excitation of the ν_{OH} mode is allowed on an ultrathin MgO film grown on Ag(100) substrate, which is not feasible on the metal substrate (**Fig. 4**).

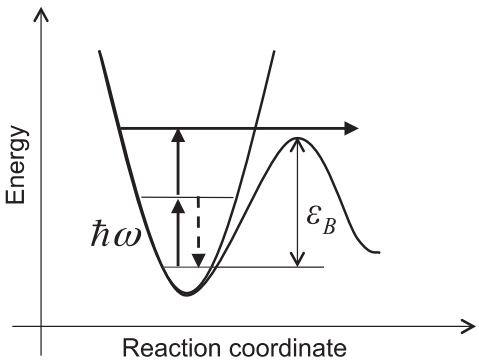

Fig. 4. Schematic energy diagram for vibrational multiple excitation via IET process on ultrathin oxide film (solid arrows). The quenching process due to short lifetime of vibrationally excited state on metal substrate is indicated with dashed arrow.

3. Controlling Water Dissociation on an Ultrathin MgO Film by Tuning Film Thickness

We performed periodic DFT calculations in order to examine how chemical activity for water dissociation on an ultrathin MgO film supported by the Ag(100) substrate.[6] As shown in **Fig. 5**, the reaction mechanism for H_2O dissociation on ultrathin MgO film surface is in agreement with that on the MgO(100) bulk surface[20] Fig. 5 a shows the energy diagram for the dissociation of a H_2O molecule on a n-ML MgO/Ag(100) ($n = 1$, 2 and 3) and on a bulk MgO(100) at the single-molecule level, which clearly indicates that the chemical activity of the ultrathin MgO film strongly depends on the film thickness. Whereas non-dissociative molecular adsorption energies, E (**A**), for the MgO films present a small variation ($< \sim 0.03$ eV) from that of bulk MgO independent of film thickness, the dissociative adsorption energy, E(**D**), is largely reduced as the film thickness decreases. The H_2O dissociation on the 1- and 2-ML MgO film is much more amenable than that on bulk MgO by 0.73 and 0.36 eV, respectively. The barrier heights (E_a) for the 1- and 2-ML MgO also considerably decrease depending on the film thickness compared to that of the bulk MgO. On the other hand, the energy profile for the 3-ML MgO film shows no significant difference from that for the bulk MgO. These computational results clearly indicate that chemical activity on ultrathin MgO films for H_2O dissociation can be tuned by film thickness as observed in the STM experiment of previous section.[9] According to the computational result, the dissociation barrier for H_2O dissociation on the 3-ML MgO film is much higher than that on the 2-ML film, and thus at least the triple excitation in the ν_{OH} mode is required to overcome it, at the single-molecule level.

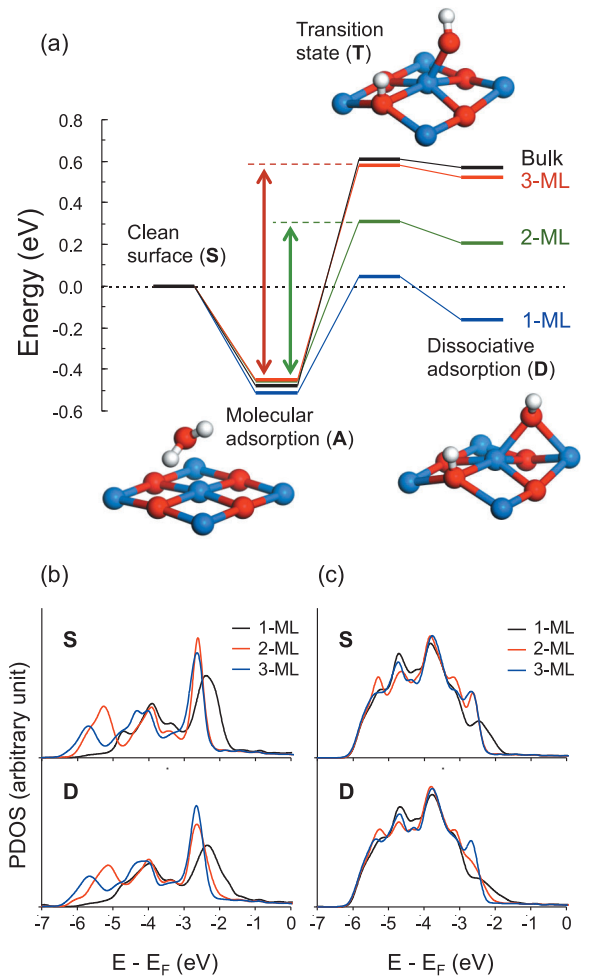

Fig. 5. (color online). (a) The energy diagram for the dissociation of a water single molecule on MgO(n-ML)/Ag(100) ($n = 1$, 2, and 3) and MgO(100) surfaces and the corresponding atomic structures for $n = 2$ (H, white ; O, red ; Mg, blue). The energy for each step is evaluated relative to the clean surface, i.e., E (H_2 O) + E (Substrate) = 0 eV. (b) PDOS of the z component of (b) O 2p and (c) Ag 4d states for MgO(n-ML)/Ag(100) ($n = 1$, 2, and 3) before water adsorption (**S**) and at a dissociative adsorption step (**D**). PDOS are plotted for the oxide-metal interface region (MgO 1 layer + Ag 2 layers). Adapted with permission from Ref. 6). Copyright 2010 American Physical Society.

Moreover, it is noteworthy that dissociation of single H_2O molecule on the 1-ML MgO film is thermodynamically exothermic regardless of either the existence of neighboring H_2O molecules or the surface defects, which are known to induce the dissociation of H_2O molecule on the MgO(100) bulk surface.[21, 22] Not only the exothermic dissociation energy but also the relatively low E_a for H_2O dissociation on the 1-ML MgO film reasonably support recent experimental observations that defect-free terrace sites on an MgO film can enhance overall chemical reactivity.[23]

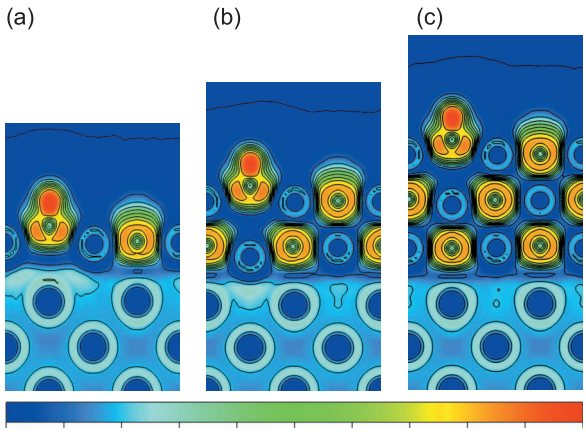

Fig. 6. (color online). ELF maps for hydroxyl ion produced by bonding between dissociated proton and surface oxygen atom at a dissociative adsorption step (**D**) for (a) 1-, (b) 2-, and (c) 3-ML MgO film. Color and contour grid for the probability of finding the electron varies from 0 (blue) to 1 (red). Adapted with permission from Ref. 6). Copyright 2010 American Physical Society.

To clarify the thickness dependence of chemical reactivity observed in H_2O dissociation on ultrathin MgO film supported by Ag(100), the DOS for the z-component of O 2p and Ag 4d at the oxide-metal interface were examined as shown in Fig. 5 b and 5 c, respectively. The DOS plots show that the electronic states distribution for the 1-ML MgO film is significantly different from those for the 2- and 3-ML films. Due to no ionic interaction between magnesium and oxygen along the z-axis at the 1-ML MgO film, the oxygen of the 1-ML MgO layer more strongly interacts with the Ag substrate compared to those of thicker films.[24] The DOS feature at the interface is maintained during non-dissociative molecular adsorption of the H_2O molecule (not shown here). However, after the dissociation on the 1- and 2-ML MgO films, the DOS tails near Fermi level (E_F) broaden as shown in Fig. 5 b and 5 c, which indicates the enhanced interfacial interaction. Therefore, it can be suggested that the order of electronic coupling at the oxide-metal interface plays an important role in determining the surface reactivity of ultrathin oxide film. This result can also be explained by investigating the electron localization function (ELF), which reveals the electron density change during H_2O dissociation. The distinguishable polarization of the electron density is observed at the oxide-metal interface of the 1- and 2-ML MgO/Ag(100) as shown in **Fig. 6** a and 6 b, respectively. However, no distinct feature is found in the 3-ML MgO film (Fig. 6 c). Although the

electronic coupling, i. e., hybridization of electronic states, between the MgO film and the Ag substrate is much weaker relative to the strong ionic bonding within the MgO film, electron density polarization observed in the 1- and 2-ML MgO films leads to a significant strengthening of adhesion at the interface. Therefore, the stability of dissociative adsorption state for the thinner MgO film can be enhanced due to the oxide-metal interaction at the interface.

4. Conclusion

We briefly reviewed our recent studies which clearly demonstrated that the dissociation paths of individual water molecules, i.e., $H_2O \rightarrow O^{2-} + 2H^+$ and $OH^- + H^+$, on MgO/Ag(100) can be selectively achieved by varying the energy of tunneling electrons to induce electronic and vibrational excitation, respectively. Successful achievement of state-selective dissociation of water molecules on ultrathin oxide film is closely related to the electronic decoupling of adsorbate from underneath metal substrate due to the insulating nature of oxide film. In addition, we revealed that the chemical activity of a metal-supported ultrathin oxide film can be controlled by film thickness, which is accounted for by stronger interfacial adhesion at the thinner oxide film. We believe that our findings provide not only deeper insight into the dynamics of water molecules on insulating films but also impetus for investigating thin oxide films for a wider range of applications.

References

1) H.-J. Freund : Surf. Sci. **601**, 1438 (2007).
2) N. Nilius : Surf. Sci. Rep. **64**, 595 (2009).
3) M. Sterrer, T. Risse, U.M. Pozzoni, L. Giordano, M. Heyde, H.-P. Rust, G. Pacchioni and H.-J. Freund : Phys. Rev. Lett. **98**, 096107 (2007).
4) A. Hellman and H. Grönbeck : Phys. Rev. Lett. **100**, 116801 (2008).
5) G. Pacchioni and H. Freund : Chem. Rev. **113**, 4035 (2013).
6) J. Jung, H.-J. Shin, Y. Kim and M. Kawai : Phys. Rev. B **82**, 085413 (2010).
7) J. Jung, H.-J. Shin, Y. Kim and M. Kawai : J. Am. Chem. Soc. **133**, 6142 (2011).
8) J. Jung, H.-J. Shin, Y. Kim and M. Kawai : J. Am. Chem. Soc. **134**, 10554 (2012).
9) H.-J. Shin, J. Jung, K. Motobayashi, S. Yanagisawa, Y. Morikawa, Y. Kim and M. Kawai : Nat. Mater. **9**, 442 (2010).
10) Y.-N. Sun, L. Giordano, J. Goniakowski, M. Lewandowski, Z.-H. Qin, C. Noguera, S. Shaikhutdinov, G. Pacchioni and H.-J. Freund : Angew. Chem., Int. Ed. **49**, 4418 (2010).
11) J.D. Holladay, J. Hu, D.L. King and Y. Wang : Catal. Today **139**, 244 (2009).
12) G.E.J. Brown, V.E. Henrich, W.H. Casey, D.L. Clark, C. Eggleston, A. Felmy, D.W. Goodman, M. Grätzel, G. Maciel, M.I. McCarthy, K.H. Nealson, D.A. Sverjensky, M.F. Toney and J.M. Zachara : Chem. Rev. **99**, 77 (1999).
13) S. Schintke, S. Messerli, M. Pivetta, F. Patthey, L. Libioulle, M. Stengel, A. De Vita and W.-D. Schneider : Phys. Rev. Lett. **87**, 276801 (2001).
14) T. Komeda, Y. Kim, M. Kawai, B.N.J. Persson and H. Ueba : Science **295**, 2055 (2002).
15) M. Ohara, Y. Kim, S. Yanagisawa, Y. Morikawa and M. Kawai : Phys. Rev. Lett. **100**, 136104 (2008).
16) K. Morgenstern and K. -H. Rieder : Chem. Phys. Lett. **358**, 250 (2002).
17) A. Mugarza, T.K. Shimizu, D.F. Ogletree and M. Salmeron : Surf. Sci. **603**, 2030 (2009).
18) H.-C. Chang and G.E. Ewing : Phys. Rev. Lett. **65**, 2125 (1990).
19) P. Liljeroth, J. Repp and G. Meyer : Science **317**, 1203 (2007).
20) J. Carrasco, F. Illas and N. Lopez : Phys. Rev. Lett. **100**, 016101 (2008).
21) L. Giordano, J. Goniakowski and J. Suzanne : Phys. Rev. Lett. **81**, 1271 (1998).
22) F. Finocchi and J. Goniakowski : Phys. Rev. B **64**, 125426 (2001).
23) S. Altieri, S.F. Contri and S. Valeri : Phys. Rev. B **76**, 205413 (2007).
24) J. Goniakowski and C. Noguera : Interface Sci. **12**, 93 (2004).